Effect of annealing on the structural, electrical and optical properties of chemically deposited nanostructured Sb_2S_3 thin films

A. U. UBALE*, T. B. GHUGARE, V. P. DESHPANDE, S. G. IBRAHIM, A. V. MITKARI, S. K. KADAM
Nanostructured Thin Film Materials Laboratory, Department of Physics, Govt. Vidarbha Institute of Science and Humanities, Amravati-444 604, Maharashtra, India

Sb_2S_3 thin films were deposited onto glass substrates at room temperature by chemical bath deposition method and annealed at 473 K temperature in air. The films were characterized for structural, surface morphological, optical and electrical properties. The X-ray diffraction analysis of the annealed film and precipitated powder showed that the deposited material is polycrystalline in nature with orthorhombic structure. The optical studies showed decrease in band-gap by 0.15 eV after annealing. The photoconductivity measurements revealed that the films were photoconducting in nature and the photoconducting character of the film increases after annealing.

(Received September 17, 2012; accepted April 11, 2013)

Keywords: Nanostructures, Thin films, Chemical synthesis, Electrical properties, Optical properties

1. Introduction

Antimony trisulfide is an important binary semiconductor useful in microwave and optoelectronic devices [1-4] particularly for electrochemical applications [5, 6]. Several investigators have prepared Sb_2S_3 thin films using different chemical methods such as Spray pyrolysis [7, 8] Chemical bath deposition (CBD) [9, 10] and Successive ionic layer adsorption and reaction method [11]. The chemical bath deposition technique is a simple and economic technique for the growth of nanostructured thin films based on bottom up concept from aqueous solution. The formation of solid phase from a solution is a two-stage process, which includes nucleation and the growth of the film. The starting chemicals are commonly available and cheap. Using this method films at low temperature can be easily prepared in order to avoid oxidation of the deposited material. The preparative parameters are easily controllable and better orientation and grain structure can be obtained [12].

The high absorption coefficient ($\alpha > 10^3$ cm^{-1}) and optimum band-gap (E_g = 1.8 eV) of Sb_2S_3 make it suitable for photovoltaic applications. Before fabrication of such devices, it is necessary to determine the structural, electrical and optical characteristics of the films and investigate impact of temperature on it. A study of these properties and their dependence on the temperature presents a great importance in order to obtain films that are capable to assure a high and stable efficiency of their respective devices. In the present investigation, films of Sb_2S_3 were prepared by CBD method at room temperature using antimony trichloride and sodium thiosulphate as antimony and sulpher source. Comparison of the structural, electrical, and optical properties of deposited Sb_2S_3 films and annealed one is discussed: in particular X-ray diffraction, electrical resistivity, photoconductivity and optical absorption. Optical absorption was used to find optical band-gap energy of deposited and annealed films.

2. Experimental

2.1. Substrate cleaning

The cleaning of glass substrate is a very important step in film deposition by CBD method. The glass substrates were boiled in chromic acid for two hours and then kept in it for 48 hours. These slides were then cleaned with dilute hydrochloric acid followed by detergent and distilled water and finally dried in AR grade acetone.

2.2. Sb_2S_3 film formation

Sb_2S_3 thin films were prepared onto glass substrate using chemical bath deposition method at 303 K temperature. The reaction bath for deposition contains 20mL 0.1M antimony trichloride, 20mL 0.1M sodium thiosulphate and 32 mL 0.1M etylendiamintetraacetic acid (EDTA), which was used as complexing agent. Due care was taken to dissolve antimony trichloride in concentrated HCl completely and then diluted with double distilled water. For the preparation of the film in $SbCl_3$ solution EDTA was added to form the complex and then stirred for few seconds and then sodium thiosulphate was added in it. EDTA is an amino-derived organic compound known to be a strong hexadentate chelating agent. It forms a complex with metal ions and dissociates reversibly at a low rate. The deposition process is based on the slow release of Sb^{3+} and S^{2-} ions in the solution, which then

condenses on the substrate. The well-cleaned glass substrates were immersed vertically at the center of the reaction bath in such a way that they did not touch the walls of the beaker. After 5 h deposition time, uniform redish orange coloured films were taken out from reaction bath and washed with distilled water. The residual precipitate was collected and filtered through Whatman's filter paper. The precipitate so collected was washed with distilled water and filtered repeatedly and then dried in air using 100 Watt tungsten lamp.

2.3. Sample characterization

The structural properties of as deposited and annealed Sb_2S_3 thin films have been analyzed by X-ray diffraction (XRD) using CuKα radiation of wavelength 0.154 nm with Philips 1710 diffractogram. The microstructure of the Sb_2S_3 thin films was studied by using a scanning electron microscope JSM 610.For SEM and EDAX the films were coated with gold palladium using coating unit E-5200 and then loaded in the sample holder. The optical absorption was studied in the wavelength range 320 to 980 nm by using UV-VIS-NIR spectrophotometer Hitachi 330. The dark electrical resistivity of Sb_2S_3 film was measured using dc two-probe method. A silver paste is applied for good ohmic contact to Sb_2S_3 thin film. The area defined was 0.5 cm^2.For photoconductivity measurements silver paint electrodes were applied on the surface of the films at a separation of 0.5 cm. A variable dc power supply and 500 W tungsten lamp was used as a light source.

3. Results and discussion

3.1 Reaction mechanism

The formation of Sb_2S_3 starts when ionic product exceeds or becomes equal to the solubility product, precipitation occurs and ions combine on the substrate and in the solution to form nuclei. The complexing agent used slows down the rate of precipitation and enables the formation of Sb_2S_3 on glass substrate. Savadogo and Mandal [13] have proposed a reaction mechanism for Sb_2S_3 film formation from alkaline bath with thioactamide as S^{2-} source. On a similar line the reaction mechanism for Sb_2S_3 film formation from acidic sodium thiosulphate bath may be proposed as follows.

In aqueous solution $Na_2S_2O_3$ dissociates as,

$$Na_2S_2O_3 \rightarrow 2Na^+ + S_2O_3^{2-} \quad (1)$$

$Na_2S_2O_3$ is a reducing agent by virtue of half cell reaction,

$$6S_2O_3^{2-} \rightarrow 3S_4O_6^{2-} + 6e^- \quad (2)$$

In acidic medium dissociation of $S_2O_3^{2-}$ takes place as,

$$3S_2O_3^{2-} + 3H^+ \rightarrow 3HSO_3^- + 3S \quad (3)$$

The electrons released in equation (2) react with S as,

$$3S + 6e^- \rightarrow 3S^{2-} \quad (4)$$

The EDTA complex of Sb^{3+} from solution reacts to give Sb_2S_3 thin films as,

$$2[(EDTA)Sb]^- + 3S^{2-} \rightarrow Sb_2S_3 + 2(EDTA)^{4-} \quad (5)$$

The Sb_2S_3 thin films thickness was measured by weight difference method with sensitive microbalance and was found of the order 130 nm.

3.2 XRD studies

The crystalline quality and orientation of the Sb_2S_3 films were investigated by X-ray diffraction. The XRD pattern of deposited film did not show any sharp peak having high intensity. The broad hump in XRD is due to amorphous glass substrate. Fig. 1 shows XRD pattern of as deposited and annealed Sb_2S_3 films. The XRD of annealed Sb_2S_3 thin film shows small intensity peaks that indicating nanocrystalline nature. The XRD pattern of precipitated Sb_2S_3 powder (Fig. 1D) shows polycrystalline nature with orthorhombic structure. The observed values were compared with standard values (Table 1), which confirms orthorhombic nature (ASTM card no. 6-0474) [14]. The lattice parameters were calculated using relation,

$$\frac{1}{d_{hkl}^2} = \left(\frac{h^2}{a^2} + \frac{k^2}{b^2} + \frac{l^2}{c^2}\right) \quad (6)$$

The calculated values of a=1.123nm, b= 1.122nm and c=0.385nm agree well with the values for orthorhombic structure of Sb_2S_3.

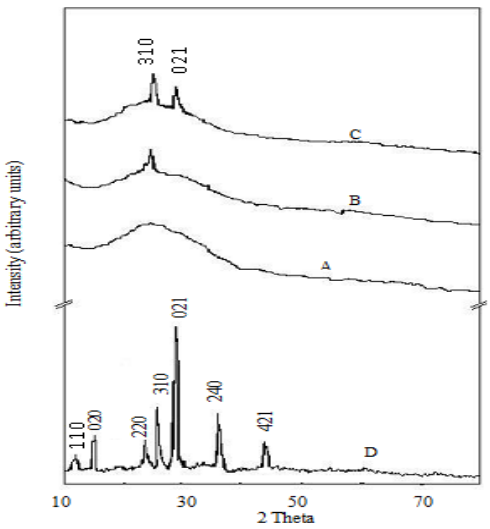

Fig 1. X-Ray diffraction patterns of Sb_2S_3 thin film of thickness 130 nm: (A) as deposited, (B) annealed at 473 K for 1 h, (C) annealed at 473 K for 2 h and (D) Precipitated powder.

Table 1. Comparison of crystallographic data for Sb_2S_3 thin films with the ASTM card no. 6-0474.

Standard data		Observed data d (A^0)		
hkl	d(A^0)	Film annealed for 1h.	Film annealed for 2h.	Precipitated powder
110	7.990	-	-	7.971
020	7.654	-	-	7.652
220	3.980	-	-	3.982
310	3.556	3.552	3.563	3.542
021	3.178	-	3.163	3.175
240	2.525	-	-	2.528
421	2.101	-	-	2.106

The average crystallite size of Sb_2S_3 film was calculated using Scherrer formula,

$$d = \frac{\lambda}{\beta \cos\theta} \quad (7)$$

Where λ is the wavelength used (0.154 nm); β is the angular line width at half maximum intensity in radians; θ is the Bragg's angle. The crystallite size of Sb_2S_3 thin film was found 17 nm after 1 hour annealing and it becomes 29 nm after 2 hours annealing, which indicates significant improvement in crystallite size after annealing in air [15, 16].

3.3 SEM studies

The surface images of the deposited and the annealed Sb_2S_3 films are shown in Fig 2. It is observed that the surface of the film is not very compact and shows round shaped clusters with distribution. A lot of empty space is observed within these clusters. The cluster size shows remarkable rise after annealing which confirms improvement in grain size.

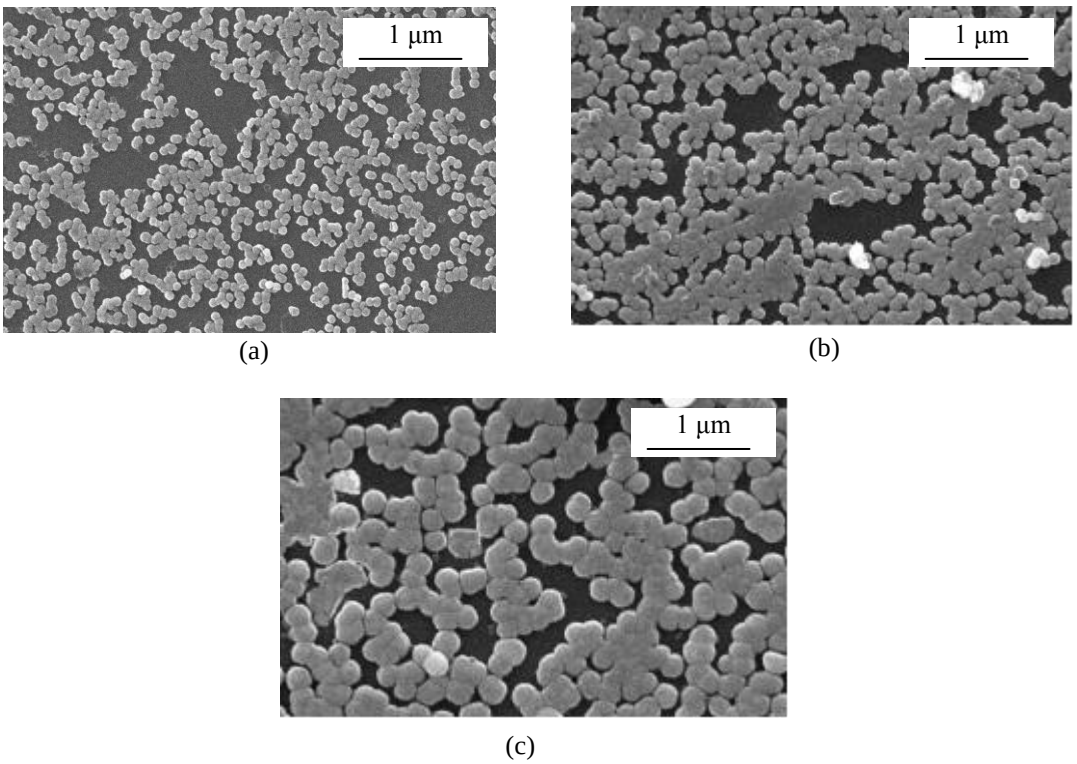

(a) (b)

(c)

Fig. 2. SEM images of Sb_2S_3 film of thickness 130nm at magnification ×20,000: (A) as-deposited (B) annealed at 473 K f or 1 h and (C) annealed at 473 K for 2 h.

The typical EDAX spectra of annealed Sb_2S_3 film is shown in Fig. 3. The elemental analysis for Sb and S shows good stoichiometry in prepared sample. The average atomic percentage of Sb:S was 39.5:61.5 showing proper formation of Sb_2S_3. The small amount of oxygen was also detected. Number of workers [17, 18] reported such accumulation of oxygen in metal sulfide thin films deposited by chemical method.

3.4 Optical absorption

An important technique for measuring the band gap energy of a semiconductor is the absorption of incident photons by the material. The photons with energies greater

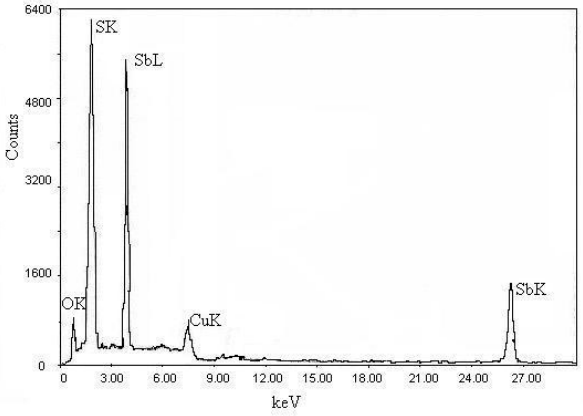

Fig. 3. Typical EDAX spectra of Sb_2S_3 thin film annealed at 473 K for1 h.

than the band gap energy are absorbed while photons with energies less than the band gap are transmitted. The absorption spectra of the deposited and the annealed Sb_2S_3 films are shown in Fig. 4. The absorption coefficient was found of the order of 10^4 cm^{-1}. In order to confirm the nature of optical transition (direct or indirect), the optical data was analyzed using the classical relation,

$$\alpha = \frac{A\left(h\upsilon - E_g\right)^n}{h\upsilon} \qquad (8)$$

where hν is the photon energy, E_g is the band gap energy, A and n are constants. For allowed direct transitions n = 1/2 for allowed indirect transitions n = 2. The plots of $(\alpha h\nu)^2$ versus hν were shown in Fig. 5. Since the variation of $(\alpha h\nu)^2$ with hν for Sb_2S_3 films is a straight line it indicates that the involved transition is direct one. Band gap energy, E_g was determined by extrapolating the straight line portion to the energy axis for zero absorption coefficient (α). The value of Eg for as deposited film was found 1.78 eV and after annealing for 1 hour and 2 hour at 473 K it becomes 1.70 and 1.63eV respectively.

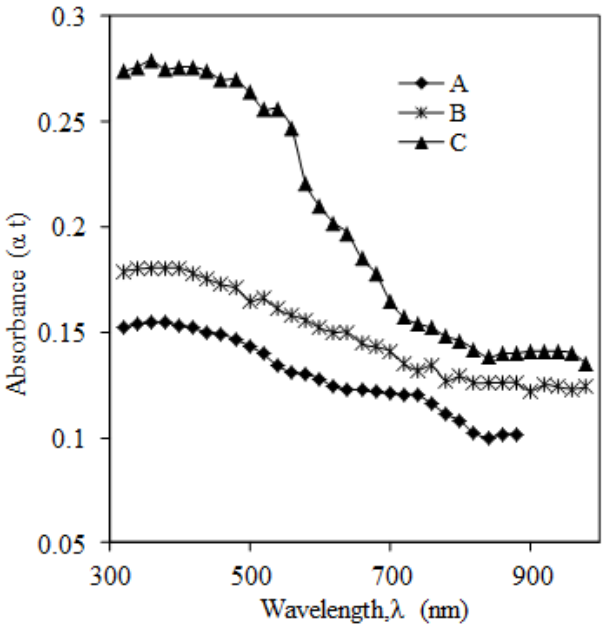

Fig. 4. Plot of optical absorption (αt) vs. wavelength for Sb_2S_3 film of thickness 130 nm: (A) as-deposited, (B) annealed at 473 K for 1 h and (C) annealed at 473 K for 2h.

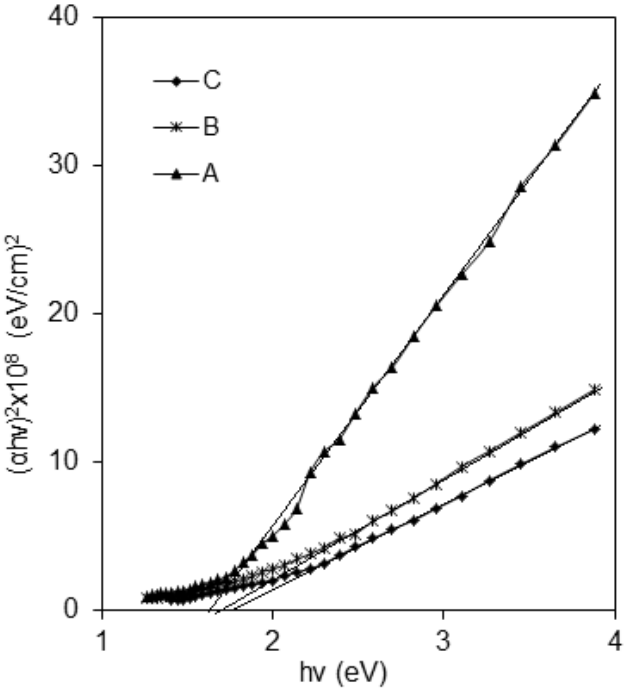

Fig. 5. Plot of $(\alpha h\nu)^2$ vs. hν for Sb_2S_3 film of thickness 130nm: (A) as-deposited, (B) annealed at 473 K for 1 h and (C) annealed at 473 K for 2 h.

The decrease in band-gap energy may be due to improvement in the crystal properties [19, 20].

3.5 Photoconductivity measurements

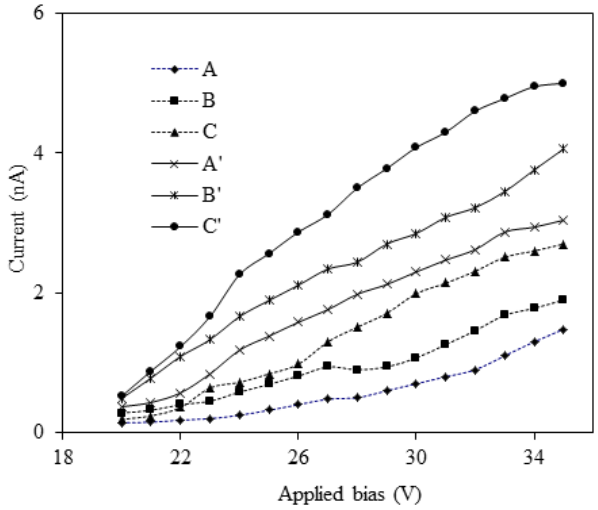

Fig. 6. IV characteristics of Sb_2S_3 film of thickness130 nm. In dark :(A) as-deposited, (B) annealed at 473 K for 1 h, (C) annealed at 473 K for 2 h. Under illumination: (A') as-deposited (B'), annealed at 473 K for 1h and (C') annealed at 473 K for 2 h.

When excess electrons and holes are produced in a semiconductor, there is a corresponding increase in the conductivity of sample. This is an important aspect, with constructive applications in the operation of several types of devices. Fig. 6 represents the current-voltage characteristics in the dark and on illumination. The difference between dark current and photocurrent is seen to increase with applied voltage. The role of barrier resistances within the grain boundaries may be responsible for the difference [21]. The photoconductivity increases after annealing remarkably. At 35V forward voltage the dark current through the film was increased by 1.56, 2.16 and 2.67 nA under illumination for the as deposited and annealed film for 1h and 2h respectively. It may be due to improvement in grain size due to annealing.

3.6 Electrical resistivity

The dc electrical resistivity of the Sb_2S_3 thin film was measured as a function of temperature in the range 303–459 K. Fig. 7 shows the variation of the dark resistivity with temperature. It is observed that the resistivity of Sb_2S_3 thin films was decreased with increase in temperature, indicating semiconducting electrical behavior. The electrical resistivity is of the order of $10^6\Omega$-cm at 303 K temperature. The thermal activation energy was calculated using the relation,

$$\rho = \rho_0 \exp (E_0/KT) \quad (9)$$

Where, ρ is resistivity at temperature T, ρ_o is a constant, K is Boltzmann constant (8.62×10^{-5} eV/K) and E_0 is the activation energy required for conduction. In the low- and high-temperature regions, activation energies are 0.31 and 0. 71 eV respectively.

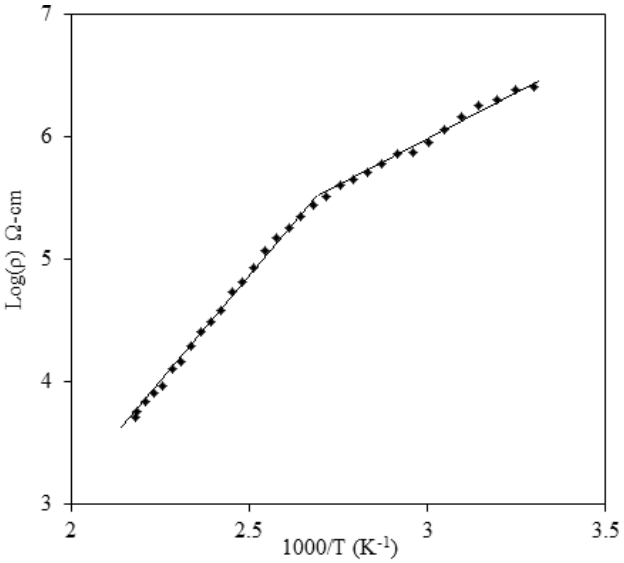

Fig. 7. Plot of variation of log of electrical resistivity with $(1/Tx10^3)$ K^{-1} of Sb_2S_3 film.

4. Conclusions

In conclusion, Sb_2S_3 thin films were prepared at room temperature from aqueous metal chloride bath using Chemical Bath Deposition method. The samples have been annealed in air to investigate the effect of air annealing on the structural, electrical and optical properties. Structural studies showed that deposited amorphous films were converted to nanocrystalline orthorhombic structure after annealing. The improvement in grain size due to annealing was also observed in SEM. A decrease in optical gap was observed after annealing.

Acknowledgement

The authors are thankful to University Grants Commission, WRO, Pune (India), for financial support under the project (No: F.47-1695/10 dated 16/3/2011).

References

[1] J. Grigas, J. Meshkanskas, J. Orlimas, Phys. Status. Solid, **A37**, 10 (1976).
[2] J. George, M. K. Radhakrishnan, Solid State Commun., **33**, 987 (1980).
[3] E. Montrimass, A. Pazera, Thin Solid Films, **34,** 65 (1976).
[4] H. Y. Lee, J. K. Keem, H. B. Chung, J. Noncryst. Solids, **279**, 209 (2001).
[5] K. Y. Rajpure, C. H. Bhosale, Mater Chem Phys, **63**(3), 263 (2000).

[6] P. K. Nair, M. T. S. Nair, V. M. Garcia, O. Arenas, Y. Pena, A. Castillo, I. Ayala, O. Gomez Daza, A. Sanchez, J. Campos, H. Hu, R. Suarez, M. E. Rincon, Solar Energy Mater. Solar Cells, **52,** 13 (1983).
[7] V. V. Killedar, C. H. Bhosale, C. D. Lokhande, Mater. Chem. Phys., **47**, 107 (1997).
[8] K. Y. Rajpure, C. H. Bhosale, C. D. Lokhande, Thin Solid Films, **311,** 114 (1997).
[9] R. S. Mane, B. R. Sankpal, C. D. Lokhande, Thin Solid Films, **353,** 29 (1999).
[10] M. T. S. Nair, Y. Pena, J. Campos, V. M. Garcia, P. K. Nair, J. Electrochem, **145,** 2113 (1998).
[11] B. R. Sankpal, H. M. Pathan, C. D. Lokhande, J. Mater. Sci. Lett., **18**, 1453 (1999).
[12] R. S. Mane, C. D. Lokhande, Mater. Chem. Phys., **65,** 1 (2000).
[13] O. Savadogo, K. C. Mandal, Solar Energy Mater. Solar Cells, **26,** 117 (1992).
[14] ASTM diffraction data file card no 6-0474.
[15] V. R. Shinde, C. D. Lokhande, R. S. Mane, S. H. Han, Appl. Surf. Sci., **245,** 407 (2005)
[16] R. Asmar, G. Ferblantier, F. Mailly, P. Gall-Borrut, A. Foucaran Thin Solid Films, **473**, 49 (2005).
[17] C. D. Lokhande, P. S. Patil, H. Tributsch, A. Ennaoui Solar Energy Mater. Solar Cells, **55**, 379 (1998).
[18] C. D. Lokhande, P. S. Patil, A. Ennaoui Appl. Surf. Sci., **123,** 294 (1998).
[19] C .Wu, R. H. Bube, J. Appl. Phys., **45**, 648 (1974).
[20] A. U. Ubale, Mater. Chem. Phys., **121**, 555 (2010).

*Corresponding author: ashokuu@yahoo.com